Dependence between the Photochemical Age Light Aromatic Hydrocarbons and the Carbon Isotope Ratios of Atmospheric Nitrophenols

Saccon, M.[1], Kornilova, A.[1], Huang, L.[2], Rudolph, J.[1]

Affiliation:

1. Centre for Atmospheric Chemistry
   York University
   4700 Keele St.
   Toronto, ON.
   M3J 1P3

2. Climate Research Division
   Atmospheric Science & Technology Directorate
   STB, Environment & Climate Change Canada
   4905 Dufferin St.
   Toronto, ON.
   M3H 5T4

Abstract

Concepts were developed to establish relationships between the stable carbon isotope ratios of nitrophenols in the atmosphere and photochemical processing of their precursors, light aromatic volatile organic compounds. The concepts are based on the assumption that nitrophenols are formed dominantly from the photo-oxidation of aromatic VOC. A mass balance model as well as various scenarios based on the proposed mechanism of nitrophenol formation were formulated and applied to derive the time integrated exposure of the precursors to processing by OH-radicals ($\int$[OH]dt) from ambient observations taken between 2009 and 2012 in Toronto, Canada. The mechanistic model included the possibility of isotopic fractionation during intermediate steps, rather than during the initial reaction step alone. This model takes into account kinetic isotope effects for reaction of the precursor VOC with the hydroxyl radical and their respective rate constants, as well as carbon isotope ratio source signatures. While many of these values are known, there were some, such as the kinetic isotope effects of reactions of first and second generation products, which were unknown. These values were predicted based on basic principles and published laboratory measurements of kinetic carbon isotope effects and were applied to the mechanistic model. Due to uncertainty of the estimates based on general principles three scenarios were used with different values for isotope effects that were not known from laboratory studies. Comparison of the dependence between nitrophenol carbon isotope ratios and $\int$[OH]dt with published results of laboratory studies and ambient observations was used to narrow the range of plausible scenarios for the mechanistic model. The results also suggests that mass balance based models do not adequately describe the dependence between nitrophenol carbon isotope ratios and $\int$[OH]dt.

1 Introduction

Secondary organic aerosols (SOA) in the atmosphere, formed from the photo-oxidation of both anthropogenic and biogenic volatile organic compounds (VOC) are poorly understood. Products formed from these reactions are only partly known and beyond the composition of SOA, little is known about its atmospheric processing. It has been proposed that the use of concentration measurements in conjunction with stable carbon isotope ratio measurements can be used to gain insight into this topic (Goldstein and Shaw, 2003; Rudolph, 2007; Gensch et al., 2014). The compounds of interest in this study are nitrophenols, which have been proposed to be formed specifically from the gas phase photo-oxidation of aromatic VOC (Forstner et al., 1997; Atkinson, 2000; Jang and Kamens, 2001; Hamilton et al., 2005; Sato et al., 2007). Once toluene, for example, is emitted from its anthropogenic sources, it is expected to react according to the proposed reaction mechanism (Forstner et al.,1997) to produce methylnitrophenols (Fig. 1). By being formed specifically from identified reactions, the stable carbon isotope ratio of the product can be linked back to the precursor and its source. Based on observations in the laboratory (Irei et al., 2011), methylnitrophenols were found to have an average isotope ratio that is close to the isotope ratio of the sum of all products calculated from mass balance.. The aqueous phase production of nitrophenols, specifically 4-nitrophenol, has also been proposed to be formed through a reaction pathway with the NO_3 radical (Hermann et al., 1995; Harrison et al., 2005). This pathway has been proposed to be a quite significant source of 4-nitrophenol in the presence of clouds with high liquid water content but has been modelled to contribute less than 2 % when the liquid water content is low (Harrison et al., 2005). Ambient measurements in the Toronto area (Saccon et al., 2015) indicate that nitrophenols are second generation products due to their depletion in ^{13}C relative to the carbon isotope ratio of the precursor.

The carbon isotope ratio of a species, which will be referred to as the delta value ($\delta^{13}C$), is defined using Eq. 1, where $(^{13}C/^{12}C)_{V\text{-}PDB}$ is the internationally accepted Vienna-Peedee Belemnite (V-PDB) value of 0.0112372. Since differences in isotope ratios between species are small, delta values are expressed in per mille notation. Limited studies using the carbon isotope ratio of atmospheric trace components, including several aromatic VOC and nitrophenols, have been applied to differentiate between sources and to trace components back to the precursor, respectively (Moukhtar et al., 2011; Kornilova et al., 2013; Saccon et al., 2013). The concept to derive information on photochemical processing of trace constituents from isotope ratios is based on the kinetic isotopic effect (KIE) which describes the dependence of the rate constant of a reaction on the atomic mass of isotopologues. In this work, the KIE will be referred to as ε (Eq. 2), where k_{12} and k_{13} are the rate constants for ^{12}C only and one ^{13}C containing isotopologues, respectively. Normal KIE, that is when ε is positive, is exhibited when a compound reacts in the atmosphere and the remaining compound is enriched in heavier isotopes, for example ^{13}C. Like delta values, ε is also expressed in per mille notation.

$$\delta^{13}C = \frac{(^{13}C/^{12}C)_{sample} - (^{13}C/^{12}C)_{V-PDB}}{(^{13}C/^{12}C)_{V-PDB}} \times 1000‰ \quad \text{Eq. 1}$$

$$\varepsilon = \frac{k_{12} - k_{13}}{k_{13}} \times 1000‰ \quad \text{Eq. 2}$$

Among other factors the concentration of a species in the atmosphere willdepend on its reactivity and the time that it has been exposed to reactants. For many VOC and semi-volatile organic compounds (SVOC) the most important reactant is the OH radical, and the time integrated OH radical concentration is often referred to as the photochemical age (PCA). The combination of laboratory experiments and ambient measurements can allow the determination of the PCA of a

specific component in SOA. The PCA for an air mass has been previously used to quantify the extent of processing of a precursor using the hydrocarbon clock by using mixing ratios of VOC (Parrish et al., 1992; Jobson et al., 1998, Jobson et al., 1999; Kleinman et al., 2003; Parrish et al., 2007). A more recently developed method uses the carbon isotope ratio of an atmospheric VOC with emissions as only relevant source, the KIE and the isotope ratio source signature to determine the PCA of this VOC. This approach is often referred to as the isotope hydrocarbon clock (Rudolph and Czuba, 2000; Rudolph et al., 2003; Thompson, 2003; Stein and Rudolph, 2007; Kornilova, 2012, Kornilova et al., 2016). The PCA of a species can be calculated using Eq. 3, where $\delta^{13}C_{pre}$ is the carbon isotope ratio of the measured ambient precursor, $\delta^{13}C_0$ is the carbon isotope ratio of the emissions, and $\int$[OH]dt is the time integrated OH concentration (PCA). It has been shown that the concept of ascribing a photochemical age to an air mass (Parrish et al., 1992) is only meaningful if all VOC emissions that contribute to the observed VOC mixing ratios have been subject to an identical extent of processing. In case of mixing air masses with VOC emissions having been subject to different extent of processing the concept of a photochemical age of an air mass has to be replaced by the concept of a photochemical age of an individual VOC (Kornilova et al., 2016). It has been shown by Rudolph and Czuba (2000) that VOC carbon isotope ratio measurements can be used to determine the concentration weighted average of the photochemical age of individual VOC provided the variability of the carbon isotope ratio of emissions is small compared to the change in carbon isotope ratio resulting from atmospheric removal reactions.

The carbon isotope ratio of the emissions of many important anthropogenic VOC precursors has been previously measured and their uncertainty typically is below 1 ‰ (Czapiewski et al., 2002; Rudolph et al., 2002; Rudolph, 2007, Gensch et al, 2014). The change in VOC mixing ratios due to reaction with OH-radicals can be described by Eq. 4, where χ_{amb} and χ_0 are the mixing

ratios of the ambient precursor and the mixing ratio that would be observed in the absence of reaction with OH-radicals, respectively. Consequently a combination of carbon isotope ratio measurements and concentration measurements allows separating between the impact of atmospheric reactions and changes in source strength or atmospheric mixing and dilution.

$$\delta^{13}C_{pre} = \delta^{13}C_0 + k_{12}\varepsilon\int [OH]dt \quad \text{Eq. 3}$$

$$\chi_{amb} = \chi_0 \exp(-k_{12}\int [OH]dt) \quad \text{Eq. 4}$$

Comparison of the difference between χ_0 and χ_{amb} with the ambient concentrations of the products of the photochemical reactions of VOC will provide insight into the yield of the secondary pollutants from the reaction. In the case of mixing air masses containing VOC with different PCA Eq. 3 still is a very good approximation for the concentration weighted average ∫[OH]dt of the precursor VOC (Rudolph and Czuba, 2000). However, Eq. 4 is only a valid approximation if the variability in PCA is small compared to the average PCA. Otherwise Eq. 4 will underestimate the average of χ_0 (Rudolph and Czuba, 2000). Consequently, yield estimates derived from combining results derived from Eq. 3 and 4 with measured ambient concentrations of reaction products will be an upper limit. In principle this limitation can be avoided by using the carbon isotope ratio of the reaction product to derive ∫[OH]dt since the average of ∫[OH]dt derived from carbon isotope ratios of the reaction products will be weighted according to the concentration of the products, which will accumulate as result of the photochemical reaction of the precursor. However, due to simultaneous formation and removal of the reaction products the relation between the carbon isotope ratio of the reaction product and the extent of photochemical processing is more complex than the simple relation between the carbon isotope ratio of the precursor and ∫[OH]dt as described by Eq. 3.

The reported carbon isotope ratio measurements of nitrophenols in the solid and the gas phase by Saccon et al. (2015) have shown that, although the average isotope ratios are consistent with laboratory studies, a significant number of delta values are between 2 ‰ to 3 ‰ lower than predicted from mass balance. This difference cannot be explained by the uncertainty of the carbon isotope ratios of precursor emission or measurements error. However, a simple mass balance only considers the KIE for the first step of the reaction mechanism, shown in Fig. 1. It must be accepted that further fractionation can occur in reaction steps following the initial reaction of the aromatic VOC with the OH-radical. In this work, we will present calculations using a mechanism based on formation and removal of nitrophenols from the atmosphere that describe the dependence between photochemical processing of light aromatic hydrocarbons and the carbon isotope ratio of nitrophenols, which are products of atmospheric reactions of light aromatic hydrocarbons. Different scenarios using a range of isotope fractionation effects for a simple mechanistic model will be discussed using the carbon isotope ratios of nitrophenols published by Saccon et al. (2015) and the laboratory studies published by Irei et al. (2015). From this comparison, the magnitude of isotope fractionation effects following the initial reaction of light aromatic VOC with OH-radicals can be constraint. PCA derived from nitrophenol carbon isotope ratios will be compared with PCA derived from carbon isotope ratios of the precursors (Kornilova et al., 2016).

2 Materials and Method

The experimental method used in this work is described in detail by Saccon et al. (2013), which is based on methods developed by Moukhtar et al. (2011) and Irei et al. (2013). The results of the carbon isotope ratio measurements have been presented by Saccon et al. (2015) and we therefore will only briefly describe the experimental procedure. Sample collection was done at

York University in Toronto, Canada using 20.32 cm x 25.4 cm quartz fiber filters (Pallflex® Tissuquartz™ filters – 2500 QAT – PallGelman Sciences) on high volume air samplers (TE-6001 from Tisch Environmental Inc.) equipped with PM2.5 heads. Uncoated quartz filters were used to collect particulate matter (PM) alone, with an average sampling time of one to three days, and filters coated with XAD-4™ resin were used for the collection of gas phase and PM, with an average sampling time of one day. Filter samples were collected between March 2009 and August 2012. The analysis of the filters included extraction in acetonitrile, and HPLC separation and solid phase extraction were used as sample clean-up steps. Concentration measurements were done using a HP 5890 GC equipped with a HP 5972 mass spectrometer; carbon isotope ratio measurements were done using a Micromass Isoprime IRMS (Isomass Scientific, Inc.). Method performance characteristics are given in Saccon et al. (2013) and Saccon et al. (2015).

3 Determination of PCA

Laboratory experiments studying the carbon isotope ratios of secondary particulate organic matter (POM) formed by the gas phase oxidation of toluene showed that the $\delta^{13}C$ value of total secondary POM can be approximated by mass balance (Irei et al., 2006, 2011). However, compound specific measurements also indicate that in some cases detailed mechanistic considerations are required to explain the observed $\delta^{13}C$ values of secondary phenols that are lower than expected from mass balance alone (Irei et al., 2015).

3.1. PCA from Mass Balance

Mass balance calculations allow a straightforward determination of the dependence between $\delta^{13}C$ of the total of secondary POM and PCA. This requires the assumption that in the atmosphere the carbon isotope ratio of the gas phase reaction products is identical to the carbon

isotope ratio of secondary POM as observed in laboratory studies (Irei et al., 2006, 2011). Furthermore, for compound specific carbon isotope ratio measurements it also has to be assumed that the carbon isotope ratio of the individual products is representative for the carbon isotope ratio of all secondary POM. In this case the dependence between PCA of the precursors and the product isotope ratio (Eq. 5) can be derived from Eq. 3 and Eq. 4. Here, k_{OH} is the averaged rate constant of all isotopomers of the precursor reacting with OH and for practical purposes, is equal to k_{12}.

$$\delta^{13}C_{prod} = \frac{\delta^{13}C_o - \exp(-k_{OH}\int [OH]dt)(\delta^{13}C_o + k_{OH}\varepsilon\int [OH]dt)}{1 - \exp(-k_{OH}\int [OH]dt)} \qquad \text{Eq. 5}$$

It should be noted that, similar to the conventional hydrocarbon clock, in the case of mixing of air masses with different PCA, the PCA from Eq. (5) is a combination of the PCA of the individual air masses, which is not always easy to interpret. Equation 5 also neglects possible isotope fractionation resulting from loss of secondary POM. The values for rate constants, carbon isotope ratio of precursor VOC emissions and kinetic isotope effects used are listed in Table 1.

3.2. PCA from detailed mechanistic concepts

The reaction sequence resulting in the formation of nitrophenols from oxidation of toluene proposed by Forstner et al. (1997) is shown in Fig. 1. It does not include details of the various branching reactions and alternate pathways resulting in other products or isotope fractionation due to loss reactions of secondary POM. While in many cases branching ratios are known, there is little direct knowledge on isotope fractionation resulting from branching reactions. Nevertheless, isotope effects for specific pathways can be estimated from the type of reaction and known

principles of isotope fractionation. For example, after formation of the cresol first generation product (Fig. 1), the probability that an OH radical is added to the ring is 92 % (Atkinson et al., 1980) while reaction at the phenolic OH group, which is expected to result in formation of nitrophenols, occurs for 8% of all reactions. The reaction of the phenolic OH group is expected to result in negligible carbon isotope fraction since it is a secondary isotope effect, while the OH radical addition will have a carbon isotope effect similar to that of other OH addition reactions to aromatic rings. Similarly, the main gas phase loss process of nitrophenols is expected to be through reaction with the OH radical, occurring through an OH addition to the ring greater than 80 % of the time (Bejan et al., 2007). Since an OH radical is added to the ring, fractionation typical for reaction at the 6 carbon atoms of aromatic ring is expected to occur for 80% of the loss reactions. Reaction at the alkyl group or the phenolic OH results in a much lower KIE than for addition to the aromatic ring and therefore their contribution to the KIE is negligible.

Another complication is the distribution between gas phase and PM. It is assumed that there are no chemical losses when the nitrophenols partition into PM, and that there is equilibrium between the gas and particle phases. Since phase distribution processes typically have very small isotope effects, partitioning between gas phase and PM is expected to have only a marginal impact on the carbon isotope ratio. This is consistent with the findings of Saccon et al. (2015). However, partitioning will influence the loss rate for SVOC since it is assumed that there is little to no chemical loss in the PM phase. It has been reported that phenols can be oxidized in aqueous solutions under conditions somewhat similar to atmospheric conditions in fog or cloud water (Yu et al., 2016). However, these reactions are very slow compared to the reaction of nitrophenols with OH-radicals in the gas phase (details see Part 1 of the Supplement). Uncertainty in phase partitioning will only result in minor uncertainties of the photochemical nitrophenol loss rate since

it has been reported that only approximately 20 % of the nitrophenols partition into the particle phase (Saccon et al., 2013, 2015). There is no information available that would allow estimating the rate of exchange of nitrophenols between gas phase and PM. It was assumed that phase partitioning is fast compared to gas phase reactions. There are indications that in some cases exchange between gas phase and PM is slower than formation or loss reactions of SVOC in the gas phase (Saccon et al., 2015), but the reported average of the difference in carbon isotope ratios between gas phase and PM is negligible (0.3±0.5) ‰.

Reaction rate constants for which no laboratory measurements are available are estimated on the following principles.. The rate constant for 3-methyl-4-nitrophenol is estimated based on the position of its substituents on the aromatic ring relative to other isomers that have known rate constants, such as 3-methyl-2-nitrophenol and 4-methyl-2-nitrophenol. For 2,6-dimethyl-4-nitrophenol it is assumed that loss reactions due to addition of the OH radical to the aromatic ring are negligible since the nitro and hydroxyl substituents both direct reactions to positions that already are occupied by other substituents and that reaction at positions 3 or 5 is unlikely to occur. It should be noted that reaction at the phenolic OH-group of 2,6-dimethyl-4-nitrophenol will not directly impact the carbon isotope ratio since this secondary carbon isotope effect will be negligible, independent of the rate of this reaction.

Using these assumptions, a set of differential equations is derived that describe the change in concentration of the isotopologues of the precursor, the first generation product (phenols), and the second generation product, nitrophenols (Eq. 6 to 8). Here, $^{12}C_{prod/int/pre}$ and $^{13}C_{prod/int/pre}$ are the concentrations of each of the ^{12}C and ^{13}C isotopologues of the second generation nitrophenol, first generation phenolic compound and aromatic precursor, respectively. ${}_{int}^{12}Y$ and ${}_{int}^{13}Y$ are the yields of the first generation product from reaction of the precursor and ${}_{prod}^{12}Y$ and

1 ${}^{13}_{prod}Y$ the yields of nitrophenols from reaction of the phenol. . The rate constants k^{12} and k^{13} for
2 different isotopologues are calculated from rate constants and the KIE.

3

$$d^{12}C_{prod} = -{}^{12}C_{prod}k^{12}_{prod}[OH]dt + {}^{12}_{prod}Y\,{}^{12}C_{int}k^{12}_{int}[OH]dt \quad \text{Eq. 6a}$$

$$d^{13}C_{prod} = -{}^{13}C_{prod}k^{13}_{prod}[OH]dt + {}^{13}_{prod}Y\,{}^{13}C_{int}k^{13}_{int}[OH]dt \quad \text{Eq. 6b}$$

$$d^{12}C_{int} = -{}^{12}C_{int}k^{12}_{int}[OH]dt + {}^{12}_{int}Y\,{}^{12}C_{pre}k^{12}_{pre}[OH]dt \quad \text{Eq. 7a}$$

$$d^{13}C_{int} = -{}^{13}C_{int}k^{13}_{int}[OH]dt + {}^{13}_{int}Y\,{}^{13}C_{pre}k^{13}_{pre}[OH]dt \quad \text{Eq. 7b}$$

$$d^{12}C_{pre} = -{}^{12}C_{pre}k^{12}_{pre}[OH]dt \quad \text{Eq. 8a}$$

$$d^{13}C_{pre} = -{}^{13}C_{pre}k^{13}_{pre}[OH]dt \quad \text{Eq. 8b}$$

4 Details of the numerical integration of these coupled differential equations are described
5 in Part 2 of the supplement. The largest uncertainty arises from the possible isotope dependence
6 of the yields in Eq. 6 and 7, but uncertainty in kinetic isotope effects also will contribute to
7 uncertainty in the calculated carbon isotope ratio. Eq. 6 to 8 only describe the fractionation relative
8 to the carbon isotope ratio of the precursor emissions. In order to determine carbon isotope ratios
9 that can be compared with observations we use the carbon isotope ratios for emissions reported by
10 Rudolph et al. (2002). To obtain insight into the possible impact of uncertainties in model
11 parameters we use different scenarios.

12 Since the yields of nitrophenols from the reaction of light aromatic VOC are small, the
13 feedback of differences in yields for isotopologues of the product on the carbon isotope ratio of
14 the first generation product is very small. It cannot be distinguished if the isotope fractionation
15 occurs during formation of the first or the second generation product. The consequence is that at

low values for the PCA the reaction channel specific isotope fractionation for the formation of nitrophenols is determined by the following equation. $KIE_{For} = \frac{{}^{13}_{prod}Yk^{13}_{int}\,{}^{13}_{int}Yk^{13}_{pre}}{{}^{12}_{prod}Yk^{12}_{int}\,{}^{12}_{int}Yk^{12}_{pre}}$ Eq. 10

KIE_{For} represents the total isotope fractionation during formation of nitrophenols following the initial reaction of the precursor with the OH-radical (for details see Part 3 of the Supplement). This greatly reduces the number of scenarios that need to be considered.

The basic parameters used for solving these differential equations are listed in Table 2. The rate constants are for 298 K for consistency with published literature data available for comparison. Rate constants for this temperature are used in the determination of PCA from carbon isotope ratios of light aromatic VOC (Kornilova et al., 2016). The laboratory studies of formation of methylnitrophenols (Irei et al.,2015) from toluene were conducted at room temperature. To understand uncertainties arising from the assumptions made to estimate KIEs which have not been determined experimentally different scenarios are used. In the first scenario (Scenario 1) it is assumed that formation of nitrophenols is entirely via abstraction of a hydrogen atom from the phenolic OH group and that, since it is a secondary KIE, there is no isotope fractionation from this reaction step. It is also assumed that there is no reaction channel specific isotope fractionation for the formation of the phenolic intermediate from the precursor, This is equivalent to the assumption that ${}^{12}_{prod}Yk^{12}_{int} = {}^{13}_{prod}Yk^{13}_{int}$ and ${}^{12}_{int}Y = {}^{13}_{int}Y$.

Another scenario (Scenario 2) is based on the assumption that the isotope fractionation for formation of nitrophenols from the intermediate is identical to the fractionation for all reactions of the intermediate and that there is no reaction channel specific isotope fractionation. It should be noted that for the formation of nitrophenol from the reaction of benzene, the two scenarios will be

identical since the reaction of phenol with the OH-radical occurs predominantly via abstraction from the OH group (Atkinson et al., 1992) and it is assumed that this secondary carbon isotope effect is negligible ($k_{int}^{12} = k_{int}^{13}$). For the reactions of toluene and xylene these two scenarios represent an estimate for the upper and lower limit of carbon isotope fractionation resulting from reactions of the first generation product.

The third scenario (Scenario 3) is based on laboratory studies of the formation of nitrophenols from gas phase reactions of toluene in the presence of NO_2 (Irei et al. 2011; Irei et al., 2015) and the lower end of atmospheric observations of nitrophenol carbon isotope ratios reported by Saccon et al. (2015). Details of how these observations can be used to constrain the isotope fractionation during formation of nitrophenols from aromatic VOC and the uncertainties of these constraints are given in Part 4 of the Supplement. Scenario 3 uses an overall isotope fractionation 3 ‰ greater than in Scenario 1. It should be noted that this does not necessarily imply a specific process for the formation of lnitrophenols from phenols.

The results of the numerical integration are plotted in Fig. 2 for 2,6-dimethyl-4-nitrophenol, 4-nitrophenol, and 2-methyl-4-nitrophenol together with predictions from mass balance. For comparison the median, 10 and 90 percentiles as well as the lowest and highest carbon isotope ratios reported by Saccon at al. (2015) are also shown. For 2-methyl-4-nitrophenol the results of laboratory studies reported by Irei et al. (2015) are included.

The predictions by the mechanistic model are very similar for the methylnitrophenol isomers (see example in Fig. S1) and for a wide range of PCA the difference in predicted carbon isotope ratios between the isomers is less than the estimated accuracy of 0.5 ‰ for carbon isotope ratio measurements of methylnitrophenols (Saccon et al. 2013).

For methylnitrophenols and 2,6-dimethyl-4-nitrophenol in all three scenarios the shape of the functions describing the dependence between carbon isotope ratio and ∫[OH]dt is very similar and the difference in the intercept with the y-axis is determined by the isotope fractionation specific for the reaction channel resulting in formation of nitrophenols and the kinetic isotope effect for the reaction of the precursor as well as the carbon isotope ratio of precursor emissions.

The steep increase in $\delta^{13}C$ at low values of ∫[OH]dt is the result of the high reactivity of the phenolic first generation product and the resulting rapid increase in its carbon isotope ratio (Fig. 3). The exception is Scenario 1 for nitrophenol which assumes that the kinetic isotope effect for reaction of phenol with the OH-radical is negligible.

At high PCA the dependence between carbon isotope ratio and PCA is nearly linear, representing conditions where the first generation phenol is in quasi steady state between formation from the precursor and loss reactions (Fig. 3). The PCA (∫[OH]dt) for transition between the initial steep increase and the nearly linear range depends primarily on the reaction rate constants of the phenolic intermediates. At high values for ∫[OH]dt the slope of the dependence between $\delta^{13}C$ and ∫[OH]dt is mainly determined by the rate constant and kinetic isotope effect for the reaction of the nitrophenol with the OH-radical since most of the aromatic precursor has been consumed (Fig. 3). Nevertheless, due to the continuing formation of nitrophenols from the precursor and the increase in $\delta^{13}C$ of the precursor this slope is slightly steeper than predicted by the rate constant and kinetic isotope effect for the reaction of the nitrophenol alone. It should be noted that the carbon isotope ratios of the precursor predicted by our mechanistic model are fully consistent with the range of carbon isotope ratios of aromatic VOC in the atmosphere reported by Kornilova et al. (2016) (Fig. 3).

3.3. Comparison of predicted carbon isotope ratios with laboratory and ambient measurements

For 2,6 dimethyl-4-nitrophenol and methylnitrophenols, the lower end of mass balance predictions is substantially heavier than the lower end of ambient observations, but for methylnitrophenols mass balance predicts carbon isotope ratios well within the range of the laboratory results reported by Irei et al. (2015). The lower end of carbon isotope ratios predicted by Scenario 1 for 2,6 dimethyl-4-nitrophenol and methylnitrophenols is 3 ‰ to 4 ‰ heavier than the lower end of ambient observations reported by Saccon et al. (2015). Furthermore, six out of the seven carbon isotope ratios of methylnitrophenols observed in laboratory studies by Irei et al. (2015) are more than 2 ‰ lighter than predictions based on Scenario 1.

Scenario 3 predicts for 4-nitrophenol at small values of the precursor's PCA ($\int[OH]dt \leq 10^{11}$ s molecules cm^{-3}) that the carbon isotope ratios are lower than the lower limit of ambient observations in an urban area of Toronto (Saccon et al. 2015). Similarly, the methylnitrophenol carbon isotope ratios predicted by Scenario 2 for a $\int[OH]dt$ of less than 3×10^{10} s molecules cm^{-3} are lighter than the lowest ambient observations (Saccon et al., 2015). Kornilova et al. (2016) reports that 25 % of PCA derived from carbon isotope ratio measurements of benzene and toluene are below 1.1×10^{11} s molecules cm^{-3} and 1.6×10^{10} s molecules cm^{-3}, respectively. However, it has to be considered that for mixing air masses of different PCA, the PCA derived from carbon isotope ratios of the precursor and the reaction product based PCA are not necessarily identical (see 3.5).

For high PCA mass balance predicts a substantially lower slope for the dependence between PCA and carbon isotope ratios than all three scenarios based on a mechanistic model. This is due to the conceptual limitation of the mass balance, which does not include the change in

carbon isotope ratio resulting from atmospheric reaction of nitrophenols and consequently it cannot be expected that a mass balance can correctly predict carbon isotope ratios at high PCA.

Most of the observed nitrophenol carbon isotope ratios correspond to PCA at the lower end of PCA predicted by Scenario 3 (Figure 2). For this range a linear approximation can be used (Part 5, Supplement). The estimated accuracy of the nitrophenol carbon isotope ratio measurements published by Saccon et al. (2015) is 0.5 ‰. This corresponds to uncertainty in ∫[OH]dt in the range of 6×10^9 s molecules cm^{-3} and 9×10^9 s molecules cm^{-3}. This is similar to the sensitivity of ∫[OH]dt derived from measurement of carbon isotope ratios of toluene (Kornilova et al., 2016). However, for PCA derived from nitrophenol carbon isotope ratios uncertainty of model predictions will also contribute to the overall uncertainty. The overall uncertainty can be described an uncertainty independent of PCA and a contribution proportional to the PCA. Detailed estimates of uncertainty are given in Part 6 of the Supplement.

3.4. PCA determined from carbon isotope ratios of nitrophenols

Based on the dependence between PCA and carbon isotope ratio of VOC reaction products (Fig. 3) ∫[OH]dt can be determined from measured carbon isotope ratios of ambient nitrophenols under the assumption of a uniform PCA of the observed nitrophenols. The average PCA determined from product carbon isotope ratios are compared in Table 3 with ∫[OH]dt values calculated directly from precursor isotope ratios, which have been published by Kornilova (2012) and Kornilova et al. (2016). The nitrophenol derived PCA is based on Scenario 3. It should be noted that, although collected at locations only 3 km apart, precursor and product samples were in most cases not collected simultaneously, and in some cases even in different years. Nevertheless,

the substantial number of samples in most of the data sets and the low uncertainty of the mean PCA justify a comparison of averages and distribution of precursor derived PCA with $\int$[OH]dt values calculated from second generation product carbon isotope ratios.

Similar to precursor carbon isotope ratio based PCA the product isotope ratio derived PCA increase substantially with decreasing precursor reactivity. This has been explained by Kornilova et al. (2016) by mixing of air masses with different PCA, which results in a lower weight for VOC with high reactivity in aged air due to faster photochemical removal. However, the weighting of contributions from different air masses differs between precursor isotope ratio derived PCA and product isotope ratio derived PCA. Details will be discussed in Section 3.5.

All precursor carbon isotope ratio derived PCA differ significantly from the PCA determined from nitrophenol carbon isotope ratios. Toluene and xylene precursor derived PCA are lower than second generation product derived PCA by approximately 4×10^{10} s molecules cm^{-3} and 3×10^{10} s molecules cm^{-3}, respectively. The average PCA derived from 4-nitrophenol carbon isotope ratios is approximately 50 % higher than the average PCA calculated from benzene carbon isotope ratios.

Uncertainty of the calculated average PCA can result from uncertainty of parameters used to calculate PCA from carbon isotope ratios. The 10 percentiles and the 90 percentiles of the second generation product carbon isotope ratios range from approximately -36 ‰ to -31 ‰. For this range errors of rate constants and kinetic isotope effects for reactions of the precursors or the second generation product only have a small impact on the dependence between PCA and carbon isotope ratio (Fig. S2 and S3) and therefore cannot explain the difference in average PCA. However, uncertainties in the carbon isotope ratios of VOC emissions as well as the isotope

fractionation for reactions or branching of the intermediates in the reaction sequence resulting in nitrophenol formation can have a significant impact on PCA calculated from nitrophenol carbon isotope ratios (Table S5, S6).

However, PCA derived from precursor's carbon isotope ratio measurements also strongly depend on the carbon isotope ratios of the emissions (Kornilova et al., 2016). For a decrease in emission isotope ratios of 1 ‰ the PCA derived from carbon isotope ratios of benzene, toluene and m-xylene increase by 0.9×10^{11} s molecules cm^{-3}, 0.3×10^{11} s molecules cm^{-3}, and 0.09×10^{11} s molecules cm^{-3}, respectively. Consequently, a decrease in the carbon isotope ratio of emission by 1 ‰ would reduce the difference between precursor and product derived PCA for benzene, toluene and xylene by approximately 0.7×10^{11} s molecules cm^{-3}, 0.15×10^{11} s molecules cm^{-3}, and less than 0.01×10^{11} s molecules cm^{-3}, respectively. An approximately 3 ‰ decrease in the carbon isotope ratio of toluene emissions would be able to explain the difference in PCA derived from toluene carbon isotope ratios and methylnitrophenol carbon isotope ratios. Similarly, an increase in the carbon isotope ratio of benzene emissions by 2.5 ‰ would eliminate the difference between benzene and 4-nitrophenol derived PCA. However, a 2-3 ‰ error in the carbon isotope ratio of emissions is substantially larger than the uncertainty derived from VOC emission studies (Rudolph et al., 2002; Rudolph, 2007; Kornilova et al., 2016). Moreover, a carbon isotope ratio of benzene emissions heavier by 2.5 ‰ than the value used in our calculations (Table 2) would not be compatible with the lower end of ambient benzene carbon isotope ratios reported by Kornilova et al. (2016). The discrepancies between the m,p-xylene and 2,6-dimethyl-4-nitrophenol derived PCA cannot be explained by uncertainty of the carbon isotope ratios of xylene emissions. However, it should be noted that the precursor based PCA is derived from ambient observations

of the combined isotope ratios of p-xylene and m-xylene, whereas only m-xylene is precursor of 2,6-dimethyl-4-nitrophenol.

An increase in the carbon isotope fractionation specific for the formation of nitrophenols from the intermediate phenol of approximately 3 ‰ would result in very good agreement between precursor and second generation product derived PCA for toluene and xylene. However, for the conditions of the laboratory studies reported by Irei et al. (2015) a model with such an additional isotope fractionation for the formation of nitrophenols from reaction of the intermediate would predict carbon isotope ratios on average by 2.5 ‰ lighter than the measured values. Based on the reported average experimental uncertainty of less than 1 ‰ this difference is significant at a higher than 99.9 % confidence level.

For the formation of 2,6-dimethyl-4-nitrophenol from m-xylene no laboratory results are available, which would allow constraining carbon isotope fractionation for reactions of the intermediate phenol. However, it is unlikely that carbon isotope fractionation for reactions of the intermediate dimethyl phenol are substantially larger than for the cresol intermediates.

The formation of 4-nitrophenol from atmospheric oxidation of benzene proceeds via phenol, which reacts with OH-radicals, in contrast to methyl substituted phenols, primarily by H-abstraction from the phenol group. Consequently, a reaction channel specific carbon isotope fractionation substantially different from that for reactions of methyl-substituted phenols cannot be ruled out. However, a model scenario that would result in good agreement between precursor and second generation product derived average PCA for benzene would also predict that the lowest

carbon isotope ratio for 4-nitrophenol exceedsapproximately 30 % of the measured ambient carbon isotope ratios reported by Saccon et al. (2015) by more than the measurement uncertainty.

In addition to the formation of nitrophenols via OH-radical initiated oxidation, reaction of the intermediate cresol with NO_3 also has to be considered a possible reaction pathway for the formation of the methylnitrophenols (Carter et al., 1981). Here, it was proposed that at NO_x levels greater than 20 ppb and ozone levels much larger than NO levels, the reaction with NO_3 would dominate over the proposed reaction with OH-radicals. However, since [OH] and [NO_3] each exhibit very pronounced diurnal cycles, with [OH] peaking during the day and [NO_3] peaking at night due to its fast photolysis during daytime, reactions with NO_3 during the day can be ignored. The proposed reaction pathway of the cresol + NO_3 reaction is through an addition reaction, resulting in a similar estimated KIE as the addition of the OH group. Consequently, the carbon isotope ratio of nitrophenols formed via this reaction pathway will not depend significantly on the formation pathway. However, due to the possible nighttime processing of the phenolic intermediate in the presence of NO_3 this may create a difference between the true value for $\int$[OH]dt and the PCA derived from the carbon isotope ratio of the nitrophenol. To determine this possible bias Scenario 3 was modified. At a value for $\int$[OH]dt corresponding to the average carbon isotope ratios reported by Saccon et al. (2015) the OH radical concentration was set to zero and replaced by a mechanism representing reaction of the intermediate at 1pmol mol^{-1} of NO_3 until the phenolic intermediate was nearly completely depleted. The resulting average bias in $\int$[OH]dt corresponds to less than 0.2 ‰ in carbon isotope ratio for all of the methylnitrophenol isomers when compared to the unmodified Scenario 3.

The reactions of cresols with OH-radicals is substantially faster than the formation of cresols from reaction of toluene with OH-radicals. This does not allow the build-up of high

concentrations of cresols during the day. This limits the possible role of the NO_3 reaction pathway. For the same reason it is unlikely that the NO_3 reaction pathway plays a substantial role for the formation of 4-nitrophenol or 2,6-dimethyl-4-nitrophenol.

Figure 4 shows the frequency distributions for PCA determined from the carbon isotope ratios of 4-nitrophenol (Fig. 4a) and methylnitrophenols (Fig. 4b) using Scenario 3. For comparison percentiles for PCA derived from carbon isotope ratios of benzene (Fig. 4a) and toluene (Fig. 4b) reported by Kornilova et al. (2016) are also shown. Consistent with the difference in average PCA (Table 3), PCA derived from 4-nitrophenol carbon isotope ratios are shifted approximately 2×10^{11} s molecules cm^{-3} towards higher values than PCA derived from benzene carbon isotope ratios, but the width of the two PCA distributions are very similar (Fig.4a). The PCA independent uncertainty for 4-nitrophenol carbon isotope ratio derived PCA is only 7×10^{11} s molecules cm^{-3} (Table S5), which cannot explain the difference in average PCA. The PCA dependent relative uncertainty is 32 % (Table S5). Combined with the PCA independent uncertainty this could just explain the difference in the average PCA. However, such a scenario also predicts a more than 30 % narrower distribution for 4-nitrophenol derived PCA than the best estimate. Such a distribution would be substantially narrower than the distribution of PCA derived from benzene carbon isotope ratios.

The PCA distribution derived for methylnitrophenols is, compared to the toluene derived distribution, not only shifted to lower values, but also much narrower (Fig. 4b). This discrepancy cannot be explained by the uncertainty of PCA derived from methylnitrophenol carbon isotope ratios.

3.5. Average PCA and mixing of air masses

Based on measurement of carbon isotope ratios of several aromatic VOC Kornilova et al. (2016) concluded that mixing ratios and average PCA of aromatic VOC in Toronto typically are determined by mixing of air masses with VOC of different origin and different PCA. While ∫[OH]dt determined from the carbon isotope ratios of aromatic VOC represent for all practical purposes the correct concentration weighted average PCA for the studied VOC (Rudolph and Czuba, 2000; Kornilova et al., 2016), the situation is different for PCA derived from carbon isotope ratios of VOC reaction products such as nitrophenols. In case of atmospheric mixing of VOC and VOC reaction products the PCA derived from product carbon isotope ratios can differ from ∫[OH]dt calculated for VOC isotope ratios for several reasons.

For nitrophenols with different PCA the decrease in sensitivity of the PCA-carbon isotope ratio dependence outside of the linear range will reduce the apparent PCA derived from nitrophenols compared to the VOC derived PCA. On the other hand, with increasing PCA the VOC precursor concentrations will not only decrease due to atmospheric dilution, but also due to chemical reactions, which reduces their weight for average PCA. In contrast to this nitrophenols are formed as result of precursor reactions, which will counteract the effect of atmospheric dilution. However, in contrast to light aromatic hydrocarbons the polar nitrophenols are water-soluble and are found both in the particle and gas phase (Saccon et al., 2013). Consequently, they will be removed not only by chemical reactions, but also by wet and dry deposition. Carbon isotope fractionation resulting from physical removal processes is much smaller than isotope fractionation during chemical reactions and therefore will have little direct impact on the carbon isotope ratio of nitrophenols. However, physical removal processes will reduce the contribution to nitrophenol

concentrations from aged air masses and therefore reduce the weight of aged air in samples representing air masses with different PCA. Combined, these effects have the potential to create a complex situation with substantial differences in PCA derived from precursor carbon isotope ratios compared to nitrophenol derived PCA.

Consequently, mixing of aged air with fresh emissions of light aromatic VOC can result in discrepancies between precusror carbon isotope ratio derived PCA and benzene carbon isotope ratio derived PCA. Lower values for precursor derived PCA can be expected if fresh emissions are mixed with aged air masses under conditions which allow accumulation of reaction products. (Fig. S7a). The accumulation of polar low volatility reaction products is not only limited by gas phase reactions, but also by deposition (An example . The principle of the impact of deposition on PCA is explained in Part 7 of the Supplement.

While conceptually mixing of two air masses with different PCA explains the difference in the frequency of observations of between precursor and product derived PCA, it can be expected that for urban sites a range of PCA will be a more realistic situation. For the average precursor derived PCA the distribution for individual PCA observations is known (Kornilova et al., 2016). We use these distributions to calculate the PCA distribution for 4-nitrophenol and understand the source of differences in the average PCA.

Figure 5 shows the resulting PCA distributions calculated for different depositional loss rates of 4-nitrophenol. With increasing loss by deposition, the centers of the distributions shift towards lower PCA and become narrower, which is the consequence of decreasing contributions of air-masses with high PCA. The center of the distribution resulting from a depositional loss rate five times faster than loss due to reaction with the OH-radical has its maximum at a value for

[OH]dt of approximately 5×10^{11} s molecules cm^{-3}, which is close to the average of PCA derived from observed 4-nitrophenol carbon isotope ratios (Table 3).

A comparison of calculated distributions with the carbon isotope ratio derived PCA distributions shows that not only the averages but also the widths of the distributions agree for depositional loss rates of 4-nitrophenol between three and seven times faster than reaction with the OH-radical (Fig. 6) within the statistical errors of the observations. Based on an average OH-radical concentration of 10^6 radicals cm^{-3} the 4-nitrophenol loss by deposition corresponds to a life time in the range of 6 days to 2 weeks. This is at the lower end of the atmospheric residence time of PM. However, only a small fraction of atmospheric 4-nitrophenol is found in the particle phase (Saccon et al., 2013), which explains that the atmospheric residence time of 4-nitrophenol exceeds the average residence time of particulate matter in the lower troposphere. Isotopic evidence does not allow differentiation between different processes unless the isotope fractionation resulting from these processes differ. Consequently the total atmospheric with no or very small isotope fractionation effects. To our knowledge there are no published values for wet or dry deposition rates of 4-nitrophenol. Consequently, we cannot identify the contribution of specific types of physical deposition processes. Based on current knowledge chemical reactions in the condensed phase are too slow to contribute to atmospheric loss of 4-nitrophenol (see detailed estimate in Part 1 of the Supplement).

The contribution of an air mass with a given PCA derived from 4-nitrophenol carbon isotope ratios depends on the deposition rate relative to the rate of reaction of 4-nitrophenol and the benzene precursor with the OH-radical (Part 7, Supplement). However, there is no direct connection between deposition rates and the reaction rate with OH-radicals and therefore for individual observations the ratio of depositional loss rate over the impact of OH-radical chemistry

can vary substantially. For example, during rain events it can be expected that deposition will be faster than on average whereas removal as well as formation of 4-nitrophenol due to reaction with OH-radicals will be slower.

Indeed, rain has a substantial impact on the atmospheric concentrations of nitrophenols in the particle phase as well as in the gas phase. Substantial precipitation during sampling or on the day before sampling, reduces the nitrophenol concentrations by a factor between 3 and 6 (Fig. 7a). In contrast, precipitation has no significant impact on PCA (Fig. 7b). Changes in PCA are within the uncertainty of the averages for different precipitation conditions and, except for 4-methyl-2-nitrophenol below 25%. Precipitation during or immediately before sampling reduces contributions from air masses with different PCA independent of the PCA of the air masses. This reduces the the atmospheric concentrations, but does not significantly impact the average PCA.

For the precursor of methylnitrophenols, toluene, the PCA distribution is very different from the distribution observed for benzene, the precursor of 4-nitrophenol (Kornilova et al., 2016). The average PCA for toluene is approximately only one third of the benzene PCA and the distribution peaks at PCA close to zero, indicating a strong influence from very recent toluene emissions. The different behavior of benzene and toluene is explained by the difference in reactivity and the different geographical distribution of emission sources (Kornilova et al., 2016). There are substantial sources of toluene within the area of Metropolitan Toronto, whereas most major sources of benzene are located in the surrounding regions.

The low average PCA derived from methylnitrophenol carbon isotope ratios is consistent with a dominant role of local emissions of toluene and demonstrates that air masses containing methylnitrophenols with high PCA are only of limited importance in determining the

methylnitrophenol derived PCA. This is supported by the dependence of methylnitrophenol concentrations, carbon isotope ratios and PCA on wind speed shown in Fig. 8 and 9.

Figure 8 indicates that when the maximum wind speed over the sampling period is lowest, concentrations for 2-methyl-4-nitrophenol are highest and the corresponding carbon isotope ratios are lowest, indicating that methylnitrophenols may be dominantly produced from local emissions with limited mixing. This is consistent with the observed PCA (Fig. 9), which is lowest when wind speed is lowest and increases with increasing wind speed. This can be explained by a decrease of the impact of local emissions resulting in a larger relative contribution of aged 2-methyl-4-nitrophenol originating from further away. A similar trend is observed for 3-methyl-4-nitrophenol. 4-methyl-2-nitrophenol and 2,6-dimethyl-4-nitrophenol were not considered due to the small number of samples. 4-nitrophenol did not show any systematic trend. This is consistent, with the, compared to toluene, lower reactivity of benzene, the 4-nitrophenol precursor and the lower local emission rates for benzene (Kornilova et al., 2016). Both factors will greatly diminish the role of local emission and local photochemistry on the average PCA derived from 4-nitrophenol carbon isotope ratios.

4 Summary and Conclusions

Similar to primary emissions of VOC for secondary pollutants PCAs derived from carbon isotope ratios decreases with increasing reactivity of the precursor. However, for the nitrophenols studied here the reactivity of the secondary pollutant is highly correlated to the reactivity of the primary pollutant. Consequently, the available experimental evidence does not allow distinction between the impacts of reactivity of primary or secondary pollutant. This allows probing atmospheric processing of pollutants at different timescales and consequently differentiating

between impact from local emission and long-range transport. In principle carbon isotope ratios of secondary organic pollutants provide better insight into the formation of secondary products than carbon isotope ratios of precursors. However, currently the use of carbon isotope ratios of secondary organic pollutants is limited by uncertainties and gaps in understanding of the formation mechanism and the carbon isotope fractionation during the reaction sequence.

Available ambient observations of precursor and second generation products carbon isotope ratiosprovide constraints for the parameters and their uncertainty in a mechanistic model describing the dependence between carbon isotope ratio and PCA of second generation products formed by photo oxidation of light aromatic VOC. Predictions by this mechanistic model are consistent with results of laboratory experiments studying the formation of methylnitrophenols from photo oxidation of toluene.

Mixing of air masses with nitrophenols of different values for $\int[OH]dt$ plays an important role in determining their carbon isotope ratios and needs to be considered in the interpretation of carbon isotope ratios of secondary organic pollutants and the relation between concentrations and carbon isotope ratios. Loss processes such as physical processes based on diffusion, solubility or chemical reactions such as secondary isotope effects that cause only very small isotope fractionation can still have a strong indirect impact on the carbon isotope ratio of nitrophenols if they play a major role in determining their atmospheric residence time. . Consequently, the dependence between atmospheric residence time and carbon isotope ratios of nitrophenols results in a strong dependence between average nitrophenol PCA and deposition rate. The dependence of deposition rate on factors only weakly related to photochemical reactivity of the atmosphere can explain the absence of a significant dependence between the concentration of nitrophenols and their carbon isotope ratios. Similarly, dispersion in the atmosphere has an indirect, but visible

impact not only on the concentration of nitrophenols, but also on their carbon isotope ratios. These results are based on observations in a major urban area with substantial local and regional nitrophenol precursor emissions. Due to the increasing uncertainty of the predictions of the mechanistic model with increasing PCA and the non-linearity of the dependence between nitrophenol carbon isotope ratios and PCA any extrapolation of these results to regions without substantial emission sources for the light aromatic compounds may be highly uncertain.

Acknowledgements

The authors would like to thank Darrell Ernst and Wendy Zhang from Environment & Climate Change Canada for their technical support. This research was supported financially by the Natural Sciences and Engineering Research Council of Canada (NSERC) and the Canadian Foundation for Climate and Atmospheric Sciences (CFCAS).

References

Anderson, R.S., Iannone, R., Thompson, A. E., Rudolph, J., Huang, L.: Carbon kinetic isotope effects in the gas-phase reactions of aromatic hydrocarbons with the OH radical at 296 ± 4K, Geophys. Res. Lett., 31, L15108, doi:10.1029/2004GL020089, 2004.

Atkinson, R.: Atmospheric chemistry of VOCs and NO_x, Atmos. Environ. 34, 2063-2101, 2000.

Atkinson, R. and Aschmann, S.M.: Rate constants for the gas-phase reactions of the OH radical with the cresols and dimethylphenols at 296 ± 2 K, Int. J. Chem. Kinet., 22, 59-67, 1990.

Atkinson, R., Carter, W.P.L., Darnall, K.R., Winer, A.M., Pitts, J.N. Jr.: A smog chamber and modeling study of the gas phase NO_x-air photooxidation of toluene and the cresols, Int. J. Chem. Kinet., 12, 779-836, 1980.

Atkinson, R., Aschmann, S.M. and Arey, J.: Reactions of OH and NO_3 radicals with phenol, cresols, and 2-nitrophenol at 296 ± 2 K, Environ. Sci. & Technol., 26, 1397-1403, 1992.

Bejan, I., Barnes, I., Olariu, R., Zhou, S., Wiesen, P., Benter, T.: Investigations on the gas-phase photolysis and OH radical kinetics of methyl-2-nitrophenols, Phys. Chem. Chem. Phys., 9, 5686-5692, 2007.

Calvert, J.G., Atkinson, R., Becker, K.H., Kamens, R.M., Seinfeld, J.H., Wallington, T.J., Yarwood, G.: The mechanisms of atmospheric oxidation of aromatic hydrocarbons, Oxford University Press, New York, USA, 2002.

Carter, W,P.L., Winer, A.M., Pitts, J.N. Jr.: Major atmospheric sink of phenol and the cresols. Reaction with the nitrate radical, Environ. Sci. Technol., 15, 829-831, 1981.

Czapiewski, K., Czuba, E., Huang, L., Ernst, D., Norman, A.L., Koppmann, R., Rudolph, J.: Isotopic composition of non-methane hydrocarbons in emissions from biomass burning, J. Atmos. Chem., 43, 45-60, 2002.

Forstner, H., Flagan, R. and Seinfeld, J.: Secondary organic aerosol from the photooxidation of aromatic hydrocarbons: Molecular composition, Environ. Sci. & Technol., 31, 1345-1358, 1997.

Gensch, I., Kiendler-Scharr, A. and Rudolph, J.: Isotope ratio studies of atmospheric organic compounds: principles, methods, applications and potential, Int. J. Mass Spectrom., 365-366, 206-221, 2014.

Goldstein, A. and Shaw, S.: Isotopes of volatile organic compounds: An emerging approach for studying atmospheric budgets and chemistry, Chem. Rev., 103, 5025-5048, 2003.

Grosjean, D.: Atmospheric fate of toxic aromatic compounds, Sci. Total Environ., 100, 367-414, 1991.

Gundel, L. and Herring, S.V.: Absorbing filter media for denuder-filter sampling of total organic carbon in airborne particles, Record of invention WIB 1457, Lawrence Berkeley National Laboratory, USA, 1998.

Hamilton, J., Webb, P., Lewis, A., Reviejo, M.: Quantifying small molecules in secondary organic aerosol formed during the photo-oxidation of toluene with hydroxyl radicals, Atmos. Environ., 39, 7263-7275, 2005.

Harrison, M.A.J., Heal, M.R. and Cape, J.N.: Evaluation of the pathways of tropospheric nitrophenol formation from benzene and phenol using a multiphase model, Atmos. Chem. Phys., 5, 1679-1695, doi:10.5194/acp-5-1679-2005, 2005.

Herrmann, H., Exner, M., Jacobi, H-W., Raabe, G., Reese, A., Zellner, R.: Laboratory studies of atmospheric aqueous-phase free-radical chemistry: Kinetic and spectroscopic studies of reactions of NO_3 and SO_4^- radicals with aromatic compounds, Faraday Discuss., 100, 129-153, 1995.

Inomata, S., Tanimoto, H., Fujitani, Y., Sekimoto, K., Sato, K., Fushimi, A., Yamada, H., Hori, S., Kumazawa, Y., Shimono, A., Hikida, T.: On-line measurements of gaseous nitro-organic compounds in diesel vehicle ehaust by proton-transfer-reaction mass spectrometry, Atmos. Environ., 73, 195-203, 2013.

Inomata, S., Fushimi, A., Sato, K., Fujitani, Y., Yamada, H.: 4-nitrophenol, 1-nitropyrene, and 9-nitroanthracene emissions in exhaust particles from diesel vehicles with different exhaust gas treatments, Atmos. Environ., 110, 93-102, 2015.

Irei, S., Huang, L., Collin, F., Zhang, W., Hastie, D., Rudolph, J.: Flow reactor studies of the stable carbon isotope composition of secondary particulate organic matter generated by OH-radical-induced reactions of toluene, Atmos. Environ. 40, 5858–5867, 2006.

Irei, S., Rudolph, J., Huang, L., Auld, J., Hastie, D.: Stable carbon isotope ratio of secondary particulate organic matter formed by photooxidation of toluene in indoor smog chamber, Atmos. Environ., 45, 856-862, 2011.

Irei, S., Rudolph, J., Huang, L: Compound-specific stable carbon isotope ratios of phenols and nitrophenols derivatized with N,O-bis(trimethylilyl)trifluoroacetamide, Anal. Chim. Acta, 786, 95-102, 2013.

Irei, S., Rudolph, J., Huang, L., Auld, J., Collin, F., Hastie, D.: Laboratory Studies of Carbon Kinetic Isotope Effects on the Production Mechanism of Particulate Phenolic Compounds Formed by Toluene Photooxidation: A Tool to Constrain Reaction Pathways, J. Phys. Chem, 119, 5-13, 2015.

Jang, M. and Kamens, R.: Characterization of secondary aerosol from the photooxidation of toluene in the presence of NO_x and 1-Propene, Environ. Sci. Technol., 35, 3626-3639, 2001.

Jobson, B.T., Parrish, D.D., Goldan, P., Kuster, W., Fehsenfeld, F.C., Blake, D.R., Blake, N.J., Niki, H.: Spatial and temporal variability of nonmethane hydrocarbon mixing ratios and their relation to photochemical lifetime, J. Geophys. Res., 103, 13557-13567, 1998.

Jobson, B.T., McKeen, S.A., Parrish, D.D., Fehsenfeld, F.C., Blake, D.R., Goldstein, A.H., Schauffler, S.M., Elkins, J.W.: Trace gas mixing ratio variability versus lifetime in the troposphere and stratosphere: Observations, J. Geophys. Res., 104, 16091-16113, 1999.

Kleinman, L.I., Daum, P.H., Lee, Y.N., Nunnermacker, L.J., Springston, S.R., Weinstein-Lloyd, J., Hyde, P., Doskey, P., Rudolph, J., Fast, J., Berkowit, C.: Photochemical age determinations in the Phoenix metropolitan area, J. Geophys. Res., 108, 4096, 2003.

Kornilova, A., Saccon, M., O'Brien, J.M., Huang, L., Rudolph, J.: Stable carbon isotope ratios and the photochemical age of atmospheric volatile organic compounds, Atmos. Ocean, 53, 7-13, 2013.

Kornilova, A.: Stable carbon isotope composition of ambient VOC and its use in the determination of photochemical ages of air masses, Ph.D. thesis, York University, Toronto, ON, 2012.

Kornilova, A., Saccon, M., Huang, L., Rudolph, J.: Stable carbon isotope ratios of ambient aromatic volatile organic compounds, Atmos. Chem. Phys., 16, 111755-11772, 2016

Moukhtar, S., Saccon, M., Kornilova, A., Irei, S., Huang, L., Rudolph, J.: Method for determination of stable carbon isotope ratio of methylnitrophenols in atmospheric particulate matter, Atmos. Meas. Tech., 4, 2453-2464, 2011.

Parrish, D.D., Hahn, C.J., Williams, E.J., Norton, R.B., Fehsenfeld, F.C., Singh, H.B., Shetter, J.D., Gandrud, B.W., Ridley, B.A.: Indications of photochemical histories of Pacific air masses from measurements of atmospheric trace species at Point Area, California, J. Geophys. Res., 97, 15,883-15,901, 1992.

Parrish, D.D., Stohl, A., Forster, C., Atlas, E.L., Blake, D.R., Goldan, P.D., Kuster, W.C., de Gouw, J.A.: Effects of mixing on evolution of hydrocarbon ratios in the troposphere, J. Geophys. Res., 112, D10S34, doi:10.1029/2006JD007583, 2007.

Rudolph, J.: Gas Chromatography-Isotope Ratio Mass Spectrometry, in: Volatile organic compounds in the atmosphere, edited by: Koppmann, R., Blackwell Publishing Ltd, UK, 388-466, 2007.

Rudolph, J. and Czuba, E.: On the use of isotopic composition measurements of volatile organic compounds to determine the "photochemical age" of an air mass, Geophys. Res. Letts., 27, 3865-3868, 2000.

Rudolph, J., Czuba, E., and Huang, L.: The stable carbon isotope fractionation for reactions of selected hydrocarbons with OH-radicals and its relevance for atmospheric observations in an urban atmosphere, J. Geophys. Res., 10, 29329-29346, 2000.

Rudolph, J., Czuba, E., Norman, A.L., Huang, L., Ernst, D.: Stable carbon isotope composition of nonmethane hydrocarbons in emissions from transportation related sources and atmospheric observations in an urban atmosphere, Atmos. Environ., 36, 1173-1181, 2002.

Rudolph, J., Anderson, R.S., Czapiewski, K.V., Czuba, E., Ernst, D., Gillespie, T., Huang, L., Rigby, C., Thompson, A.E.: The stable carbon isotope ratio of biogenic emissions of isoprene and the potential use of stable isotope ratio measurements to study photochemical processing of isoprene in the atmosphere, J. Atmos. Chem., 44, 39-55, 2003.

Saccon, M., Busca, R., Facca, C., Huang, L., Irei, S., Kornilova, A., Lane, D., Rudolph, J.: Method for the determination of concentration and stable carbon isotope ratios of atmospheric phenols, Atmos. Meas. Tech., 6, 2969-2974, 2013.

Saccon, M., Kornilova, A., Huang, L., Moukhtar, S., Rudolph, J.: Stable carbon isotope ratios of ambient secondary organic aerosols in Toronto, Atmos. Chem. Phys., 15, 10825-10838, 2015.

Sato, K., Hatakeyama, S., Imamura, T.: Secondary organic aerosol formation during the photooxidation of toluene: NO_x dependence of chemical composition, J. Phys. Chem. A, 111, 9796-9808, 2007.

Spivakovsky, C.M., Logan, J.A., Montzka, S.A., Balkanski, Y.J., Foreman-Fowler, M., Jones, D.B.A., Horowitz, L.W., Fusco, A.C., Brenninkmeijer, C.A.M., Prather, M.J., Wofsy, S.C., McElroy, M.B.: Three-dimensional climatological distribution of tropospheric OH: Update and evaluation, J. Geophys. Res., 105, 8931-8980, 2000.

Stein, O. and Rudolph, J.: Modeling and interpretation of stable carbon isotope ratios of ethane in global chemical transport models, J. Geophys. Res., 112, D14308, doi:10.1029/2006JD008062, 2007.

Thompson, A.: Stable carbon isotope ratios of nonmethane hydrocarbons and halocarbons in the atmosphere, Ph.D. thesis, York University, Toronto, ON, 2003.

Tremp, J., Mattrel, P., Fingler, S., Giger, W.: Phenols and nitrophenols as tropospheric pollutants: emissions from automobile exhausts and phase transfer in the atmosphere, Water Air Soil Poll., 68, 113-123, 1993.

Yu, L., Smith, J., Laskin, A., George, K.M., Anastasio, C., Laskin, J., Ann M. Dillner, A.D., Zhang,Q.: Molecular transformations of phenolic SOA during photochemical aging in the aqueous phase: competition among oligomerization, functionalization, and fragmentation, Atmos. Chem. Phys., 16, 4511–4527, 2016.

Tables

Table 1. Parameters, including the rate constant of the precursor with the OH radical (k_{OH}), KIE and the carbon isotope ratio of emissions ($\delta^{13}C_0$) used for the determination of the PCA by Eq. (5). The uncertainty of the parameter is given in parenthesis.

Precursor			Product	Product Abbreviation
Benzene	k_{OH}[a] (cm^3 $molec^{-1}$ s^{-1})	1.39×10^{-12}	4-nitrophenol	4-NP
	ε[b] (‰)	7.83 (0.42)		
	$\delta^{13}C_0$[c] (‰)	-28.0 (0.2)		
Toluene	k_{OH}[a] (cm^3 $molec^{-1}$ s^{-1})	5.63×10^{-12}	4-methyl-2-nitrophenol	4-me-2-NP
	ε[b] (‰)	5.95 (0.28)	3-methyl-4-nitrophenol	3-me-4-NP
	$\delta^{13}C_0$[c] (‰)	-27.6 (0.5)	2-methyl-4-nitrophenol	2-me-4-NP
m-Xylene	k_{OH}[a] (cm^3 $molec^{-1}$ s^{-1})	2.31×10^{-11}	2,6-dimethyl-4-nitrophenol	2,6-dime-4-NP
	ε[b] (‰)	4.83 (0.05)		
	$\delta^{13}C_0$[c] (‰)	-27.4 (0.4)		

[a] Calvert et al., 2002, uncertainty not included since the uncertainty resulting from error in the rate constants is small compared to uncertainties derived from error in the carbon isotope ratio and KIE. [b] Anderson et al. (2004). [c] Rudolph et al. (2002); for m-xylene the value reported for p+m-xylene is given.

Table 2. Parameters used to determine the PCA for individual products. Units of k (rate constant) are in cm^3 $molecule^{-1}$ s^{-1}. Since 80 % of the phenols are in the gas phase (Saccon et al., 2013), the rate constant for the product loss was adjusted to 80 % of the gas phase rate constant. If available, the uncertainty of the parameter is given in parenthesis.

Precursor			Intermediate			Product (Gas + PM)		
Benzene	k^a	1.39×10^{-12}	Phenol	k^a	2.70×10^{-11}	4-NP	k^e	3.40×10^{-13}
	$\varepsilon_{OH}{}^b$ (‰)	7.83 (0.42)		$\varepsilon_{OH}{}^d$ (‰)	0		$\varepsilon_{OH}{}^f$ (‰)	5.36
	$\delta^{13}C_0{}^c$ (‰)	-28.0 (0.2)						
Toluene	k^a	5.63×10^{-12}	4-me-phenol	k^a	5.0×10^{-11}	4-me-2-NP	k^h	2.87×10^{-12}
	$\varepsilon_{OH}{}^b$ (‰)	5.95 (0.28)		$\varepsilon_{OH}{}^g$ (‰)	5.47		$\varepsilon_{OH}{}^i$ (‰)	5.95
	$\delta^{13}C_0{}^c$ (‰)	-27.6 (0.5)						
Toluene	k^a	5.63×10^{-12}	3-me-phenol	k^a	6.8×10^{-11}	3-me-4-NP	k^j	2.92×10^{-12}
	$\varepsilon_{OH}{}^b$ (‰)	5.95 (0.28)		$\varepsilon_{OH}{}^g$ (‰)	5.47		$\varepsilon_{OH}{}^i$ (‰)	5.95
	$\delta^{13}C_0{}^c$ (‰)	-27.6 (0.5)						
Toluene	k^a	5.63×10^{-12}	2-me-phenol	k^a	4.1×10^{-11}	2-me-4-NP	k^k	2.87×10^{-12}
	$\varepsilon_{OH}{}^b$ (‰)	5.95 (0.28)		$\varepsilon_{OH}{}^g$ (‰)	5.47		$\varepsilon_{OH}{}^i$ (‰)	5.95
	$\delta^{13}C_0{}^c$ (‰)	-27.6 (0.5)						
m-xylene	k^a	2.31×10^{-11}	2,6-dime-phenol	k^l	6.59×10^{-11}	2,6-dime-4-NP	k^m	0
	$\varepsilon_{OH}{}^b$ (‰)	4.83 (0.05)		$\varepsilon_{OH}{}^g$ (‰)	4.83		$\varepsilon_{OH}{}^m$ (‰)	0
	$\delta^{13}C_0{}^c$ (‰)	-27.4 (0.4)						

[a] Reaction rate constant taken from Calvert et al., 2002. [b] Kinetic isotope effects taken from Anderson et al., 2004. [c] Carbon isotope ratio of emissions taken from Rudolph et al. (2002) and Kornilova et al. (2016); for m-xylene the value reported for p+m-xylene is given. [d] Reaction occurs via OH abstraction (Atkinson et al., 1992) and the secondary carbon isotope effect is assumed to be negligible. [e] Rate constant from Grosjean (1991). [f] Estimated based on loss reaction proceeding mostly by addition to the aromatic ring (Grosjean, 1991) and the carbon kinetic isotope effects reported by Anderson et al. (2004). [g] Estimated on the assumption that reaction proceeds primarily through an addition pathway (Atkinson et al., 1980). The kinetic isotope effect for addition of OH-radicals to an aromatic ring are based on the kinetic isotope effects reported by Anderson et al. (2004). [h] Rate constant from Bejan et al. (2007). [i] Estimate based on the carbon kinetic isotope effects for reactions of aromatic VOC reported by Anderson et al. (2004). [j] Rate constant assumed to be the average of the rate constants for 3-me-2-NP (3.69×10^{-12} cm^3 $molec^{-1}$ s^{-1}) and 4-me-2-NP reported by Bejan et al. (2007). [k] Rate constant estimated to be identical to the rate constant reported for 4-me-2-NP by Bejan et al. (2007). [l] Reaction rate constant from Atkinson and Aschmann (1990). [m] Assumed to have no loss reaction that results in carbon isotope fractionation, see text.

Table 3. Averages and uncertainty of the mean PCA for nitrophenols in both PM and in the gas phase and PM calculated for Scenario 3. Also shown are the average carbon isotope ratios. The number of data points used is shown in brackets. For comparison PCA calculated from the carbon isotope ratios of the precursor VOC reported by Kornilova et al. (2016) for Toronto are included.

Precursor	Average PCA[a] (10^{11} s molec cm^{-3})	Product	Average $\delta^{13}C$ (‰)	Average PCA (10^{11} s molec cm^{-3})
Benzene	3.1 ± 0.5 (43)	4-NP	-33.5 ± 0.3	4.7 ± 0.3 (58)
Toluene	0.85±0.11 (73)	Methyl-nitrophenols	-33.1±0.1	0.42±0.02 (120)
p,m-Xylene	0.34 ± 0.06 (56)	2,6-dime-4-NP	-33.4 ± 0.5	0.11 ± 0.04 (19)

[a] Average carbon isotope ratio and PCA determined by Kornilova (2012) and Kornilova et al., (2016)

Figure Captions

Figure 1. Proposed formation mechanism of 2-methyl-4-nitrophenol from toluene oxidation (adapted from Forstner et al., 1997).

Figure 2. Dependence between carbon isotope ratio and PCA ($\int$[OH]dt) for several nitrophenols calculated for different scenarios using a mechanistic model and mass balance. Also shown are the median, 10 and 90 percentiles as well as the lowest and highest carbon isotope ratios measured by Saccon at al. (2015) in an urban area. The triangles and squares represent the carbon isotope ratios of 3-methyl-4-nitrophenol and 2-methyl-4-nitrophenol, respectively, reported by Irei et al. (2015) for laboratory studies.

Figure 3. Dependence between carbon isotope ratio and PCA ($\int$[OH]dt) for 2-methyl-4-nitrophenol, its precursor (toluene) and the phenolic intermediate calculated for Scenario 3. Also shown are the median, 10 and 90 percentiles as well as the lowest and highest carbon isotope ratios for toluene reported by Kornilova et al. (2016) for an urban area in Toronto (Canada).

Figure 4. Frequency distribution of PCA determined from the carbon isotope ratios of 4-nitrophenol (a) and methylnitrophenols (b) using Scenario 3. For comparison the median (dotted line), 75 and 25 percentiles (dashed line) and 10 and 90 percentiles (solid line) determined by Kornilova et al. (2016) from carbon isotope ratios of benzene (a) and toluene (b) are included.

Figure 5. PCA distributions calculated for different depositional loss rates of 4-nitrophenol. The depositional loss rates are given as multiples of the chemical loss rate of 4-nitrophenol due to reaction with OH-radicals. For comparison, the PCA distribution determined from the precursor carbon isotope ratio distribution (Kornilova et al., 2016) is also shown (solid line).

Figure 6. Comparison of PCA distributions calculated for different depositional loss rates of 4-nitrophenol. The depositional loss rates are given as multiples of the chemical loss rate of 4-nitrophenol due to reaction with OH-radicals. For comparison, the PCA distribution determined from the 4-nitrophenol carbon isotope ratios reported by Saccon et al. (2015) are also shown. The error bars represent the statistical uncertainty resulting from the limited number of observations.

Figure 7. Average nitrophenol concentrations (a) and PCA (b) determined from carbon isotope ratios reported by Saccon et al. (2015) using Scenario 3 for different precipitation conditions during and before sampling. No rain: In total less than 1 mm on the day of sampling and the day before; light rain: between 1 mm and 10 mm precipitation on the day of sampling or a total of >4 mm on the day of sampling and the day before; heavy rain: > 20 mm precipitation on the day of sampling or > 10 mm on the day of sampling and > 20 mm on the day before. Precipitation data were taken from Environment Canada: Historical Data, Toronto North York site.

Figure 8. Plot of concentrations (black diamonds, left axis) and carbon isotope ratios (open diamonds, right axis) of 2-methyl-4-nitrophenol as a function of the maximum wind speed during sampling (Environment Canada: Historical Weather Data, Toronto North York Site). Points were sorted in order of increasing wind speed and each point is an average of 10 filter samples; samples collected while there was precipitation were excluded. Error bars are the errors of the mean.

Figure 9. The PCA of 2-methyl-4-nitrophenol as a function of the maximum wind speed during sampling (Environment Canada: Historical Data, Toronto North York site). Points were sorted in

order of increasing wind speed and each point is an average of 10 filter samples; samples collected while there was precipitation were excluded. Error bars are the errors of the mean.

Figures

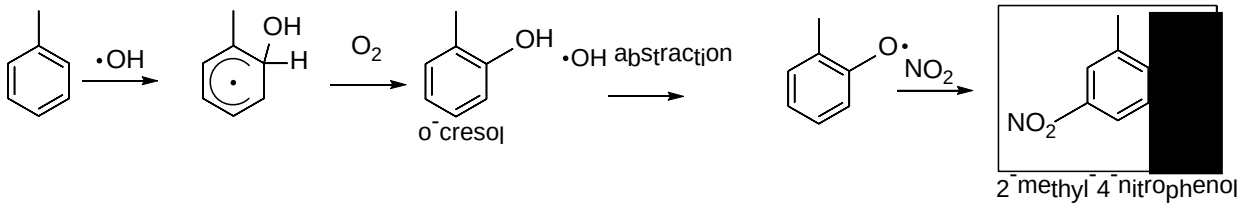

Figure 2. Proposed formation mechanism of 2-methyl-4-nitrophenol from toluene oxidation (adapted from Forstner et al., 1997).

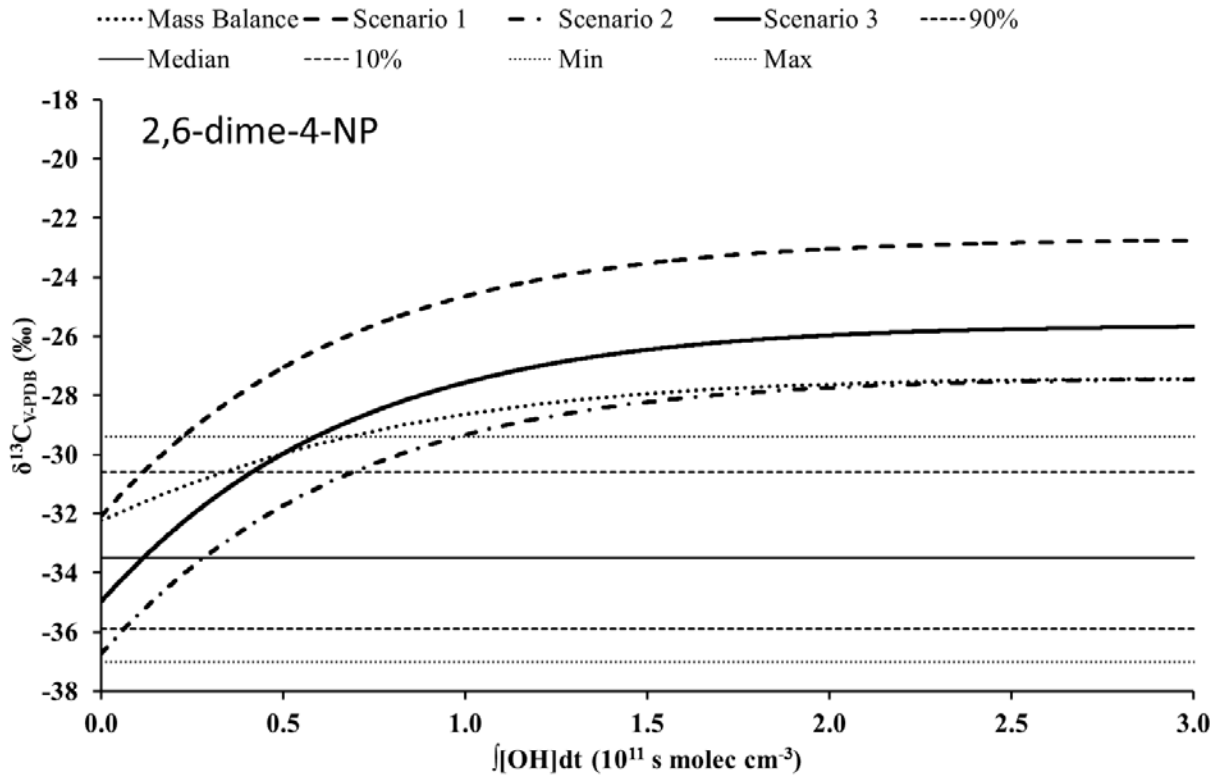

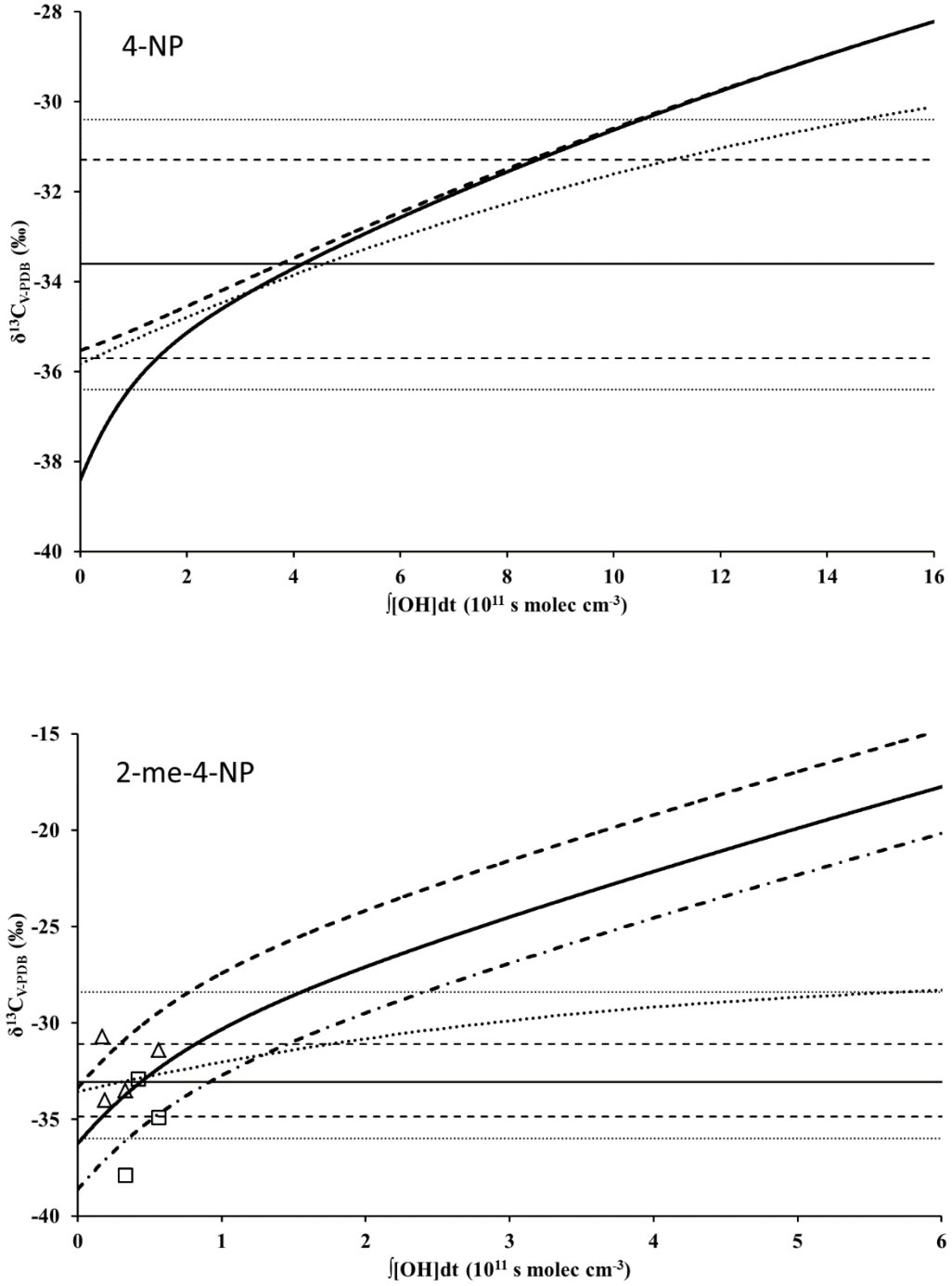

Figure 2. Dependence between carbon isotope ratio and PCA (∫[OH]dt) for several nitrophenols calculated for different scenarios using a mechanistic model and mass balance. Also shown are the median, 10 and 90 percentiles as well as the lowest and highest carbon isotope ratios measured by Saccon at al. (2015) in an urban area. The triangles and squares represent the carbon isotope ratios of 3-methyl-4-nitrophenol and 2-methyl-4-nitrophenol, respectively, reported by Irei et al. (2015) for laboratory studies.

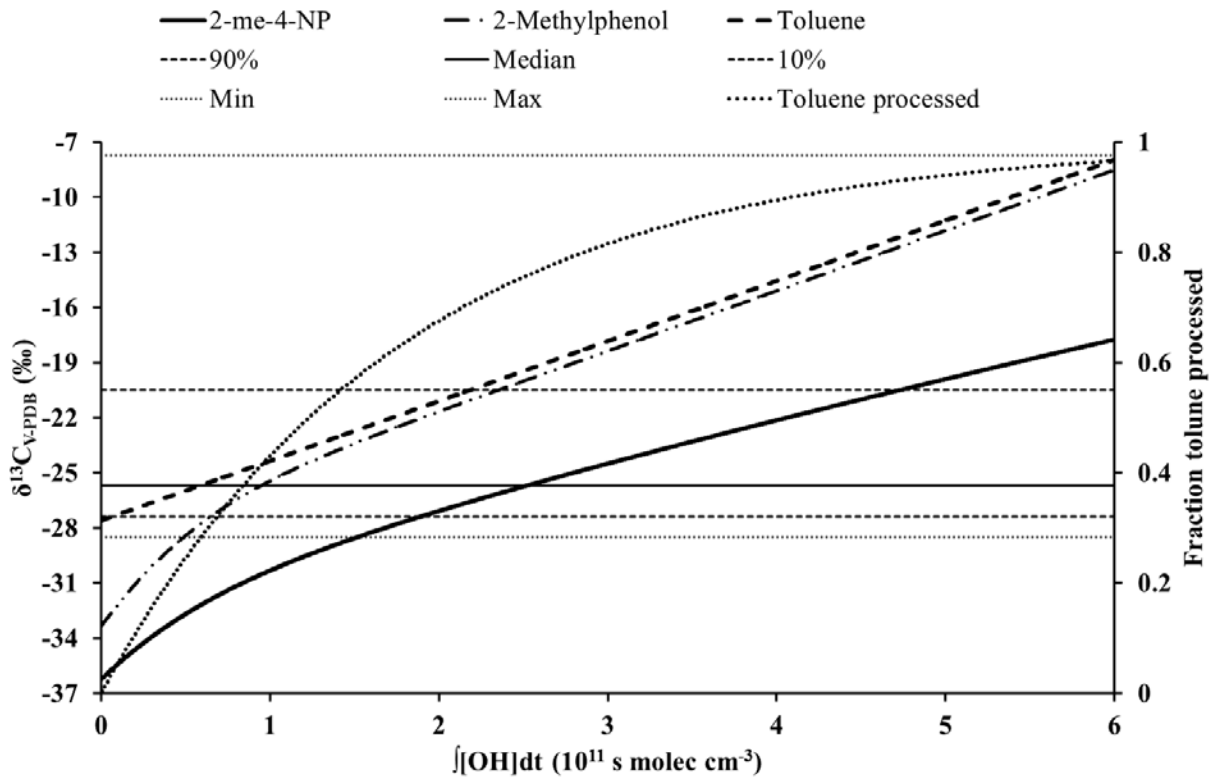

Figure 3. Dependence between carbon isotope ratio and PCA (∫[OH]dt) for 2-methyl-4-nitrophenol, its precursor (toluene) and the phenolic intermediate calculated for Scenario 3. Also shown are the median, 10 and 90 percentiles as well as the lowest and highest carbon isotope ratios for toluene reported by Kornilova et al. (2016) for an urban area in Toronto (Canada). Also shown (dotted line, secondary y-axis) is the fraction of toluene processed as function of PCA.

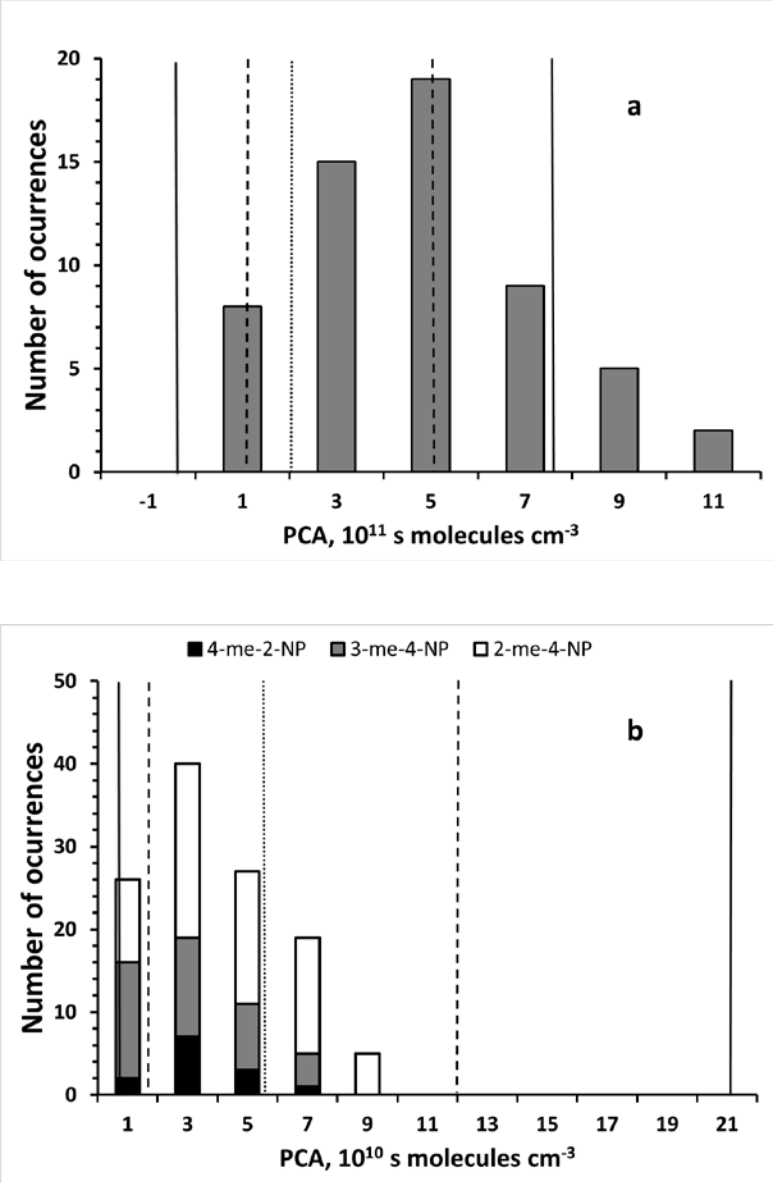

Figure 4. Frequency distribution of PCA determined from the carbon isotope ratios of 4-nitrophenol (a) and methylnitrophenols (b) using Scenario 3. For comparison the median (dotted line), 75 and 25 percentiles (dashed line) and 10 and 90 percentiles (solid line) determined by Kornilova et al. (2016) from carbon isotope ratios of benzene (a) and toluene (b) are included.

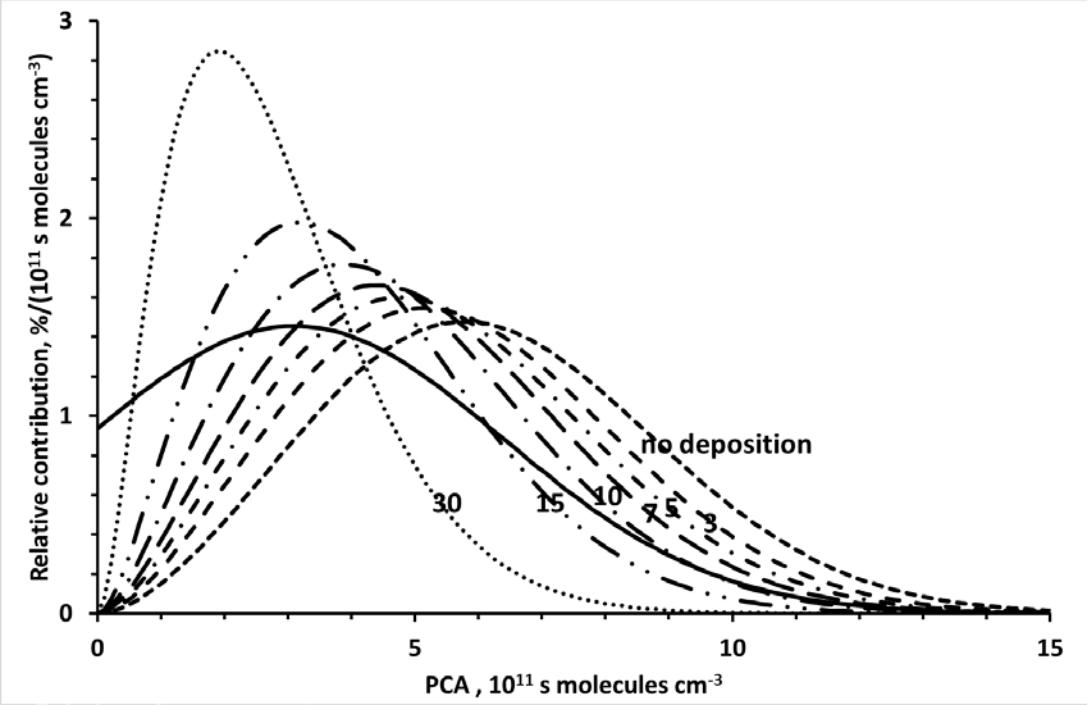

Figure 5. PCA distributions calculated for different depositional loss rates of 4-nitrophenol. The depositional loss rates are given as multiples of the chemical loss rate of 4-nitrophenol due to reaction with OH-radicals. For comparison, the PCA distribution determined from the precursor carbon isotope ratio distribution (Kornilova et al., 2016) is also shown (solid line).

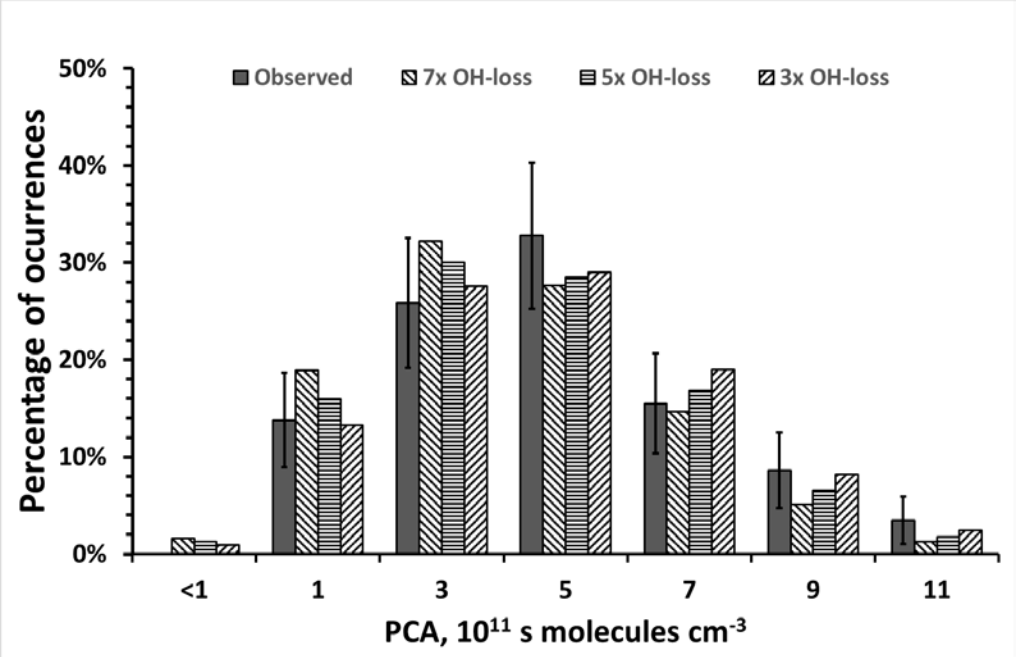

Figure 6. Comparison of PCA distributions calculated for different depositional loss rates of 4-nitrophenol. The depositional loss rates are given as multiples of the chemical loss rate of 4-nitrophenol due to reaction with OH-radicals. For comparison, the PCA distribution determined from the 4-nitrophenol carbon isotope ratios reported by Saccon et al. (2015) are also shown. The error bars represent the statistical uncertainty resulting from the limited number of observations.

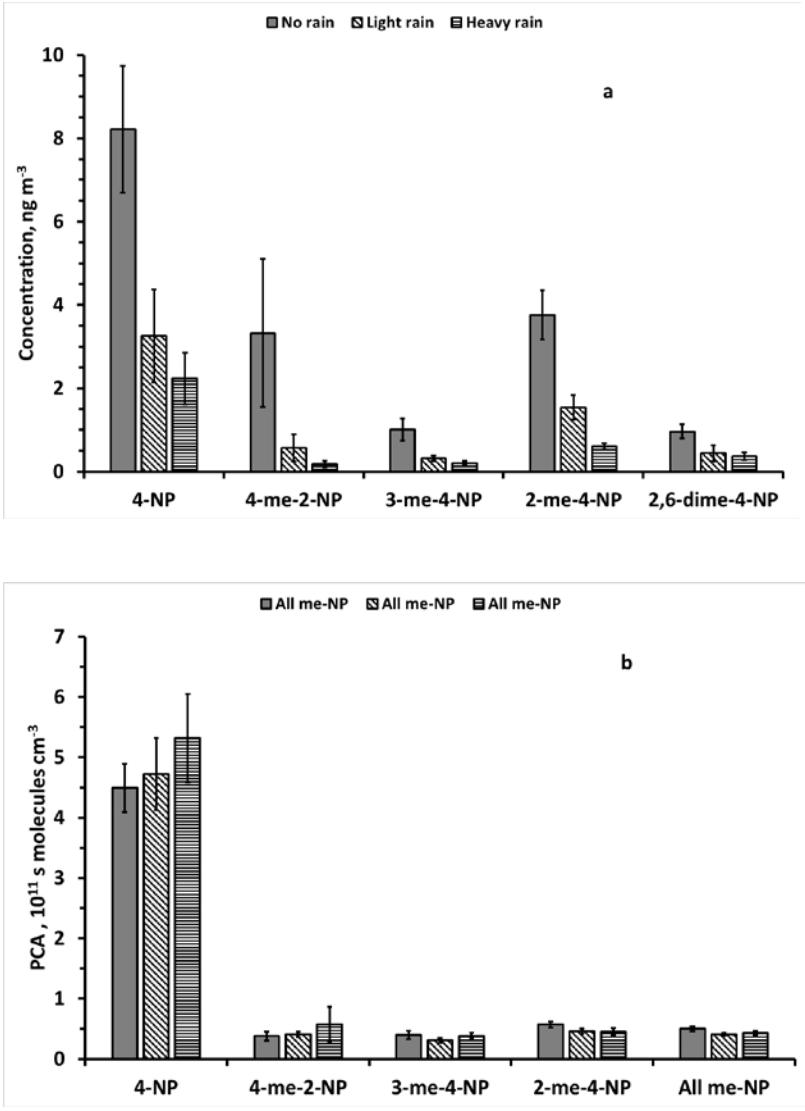

Figure 7. Average nitrophenol concentrations (a) and PCA (b) determined from carbon isotope ratios reported by Saccon et al. (2015) using Scenario 3 for different precipitation conditions during and before sampling. No rain: In total less than 1 mm on the day of sampling and the day before; light rain: between 1 mm and 10 mm precipitation on the day of sampling or a total of >4 mm on the day of sampling and the day before; heavy rain: > 20 mm precipitation on the day of sampling or > 10 mm on the day of sampling and > 20 mm on the day before. Precipitation data were taken from Environment Canada: Historical Data, Toronto North York site.

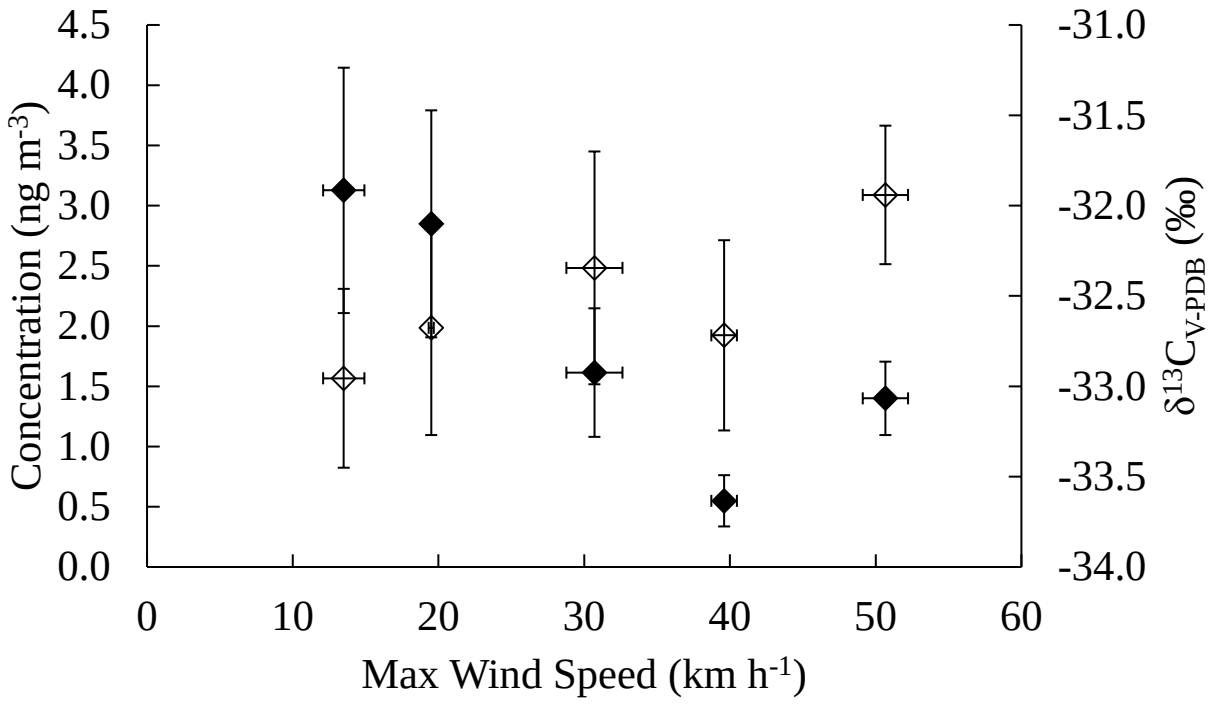

Figure 8. Plot of concentrations (black diamonds, left axis) and carbon isotope ratios (open diamonds, right axis) of 2-methyl-4-nitrophenol as a function of the maximum wind speed during sampling (Environment Canada: Historical Weather Data, Toronto North York Site). Points were sorted in order of increasing wind speed and each point is an average of 10 filter samples; samples collected while there was precipitation were excluded. Error bars are the errors of the mean.

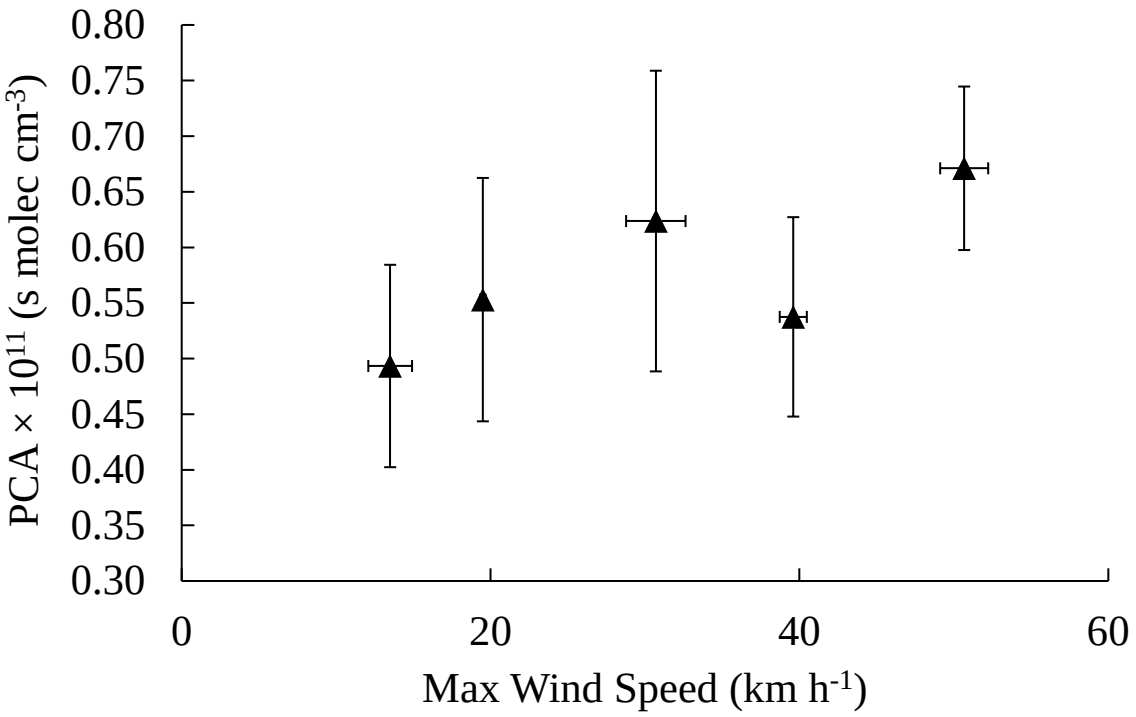

Figure 9. The PCA of 2-methyl-4-nitrophenol as a function of the maximum wind speed during sampling (Environment Canada: Historical Data, Toronto North York site). Points were sorted in order of increasing wind speed and each point is an average of 10 filter samples; samples collected while there was precipitation were excluded. Error bars are the errors of the mean.